

Journal Pre-proof

Automatic analysis of skull thickness, scalp-to-cortex distance and association with age and sex in cognitively normal elderly

Junhao Zhang, Valerie Treyer, Junfeng Sun, Chencheng Zhang, Anton Gietl, Christoph Hock, Daniel Razansky, Roger M. Nitsch, Ruiqing Ni, for the Alzheimer's Disease Neuroimaging Initiative

PII: S1935-861X(23)01711-4

DOI: <https://doi.org/10.1016/j.brs.2023.03.011>

Reference: BRS 2349

To appear in: *Brain Stimulation*

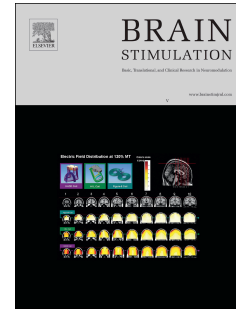
Received Date: 5 March 2023

Accepted Date: 21 March 2023

Please cite this article as: Zhang J, Treyer V, Sun J, Zhang C, Gietl A, Hock C, Razansky D, Nitsch RM, Ni R, for the Alzheimer's Disease Neuroimaging Initiative, Automatic analysis of skull thickness, scalp-to-cortex distance and association with age and sex in cognitively normal elderly, *Brain Stimulation* (2023), doi: <https://doi.org/10.1016/j.brs.2023.03.011>.

This is a PDF file of an article that has undergone enhancements after acceptance, such as the addition of a cover page and metadata, and formatting for readability, but it is not yet the definitive version of record. This version will undergo additional copyediting, typesetting and review before it is published in its final form, but we are providing this version to give early visibility of the article. Please note that, during the production process, errors may be discovered which could affect the content, and all legal disclaimers that apply to the journal pertain.

© 2023 Published by Elsevier Inc.



Automatic analysis of skull thickness, scalp-to-cortex distance and association with age and sex in cognitively normal elderly

Junhao Zhang^{1,2}, Valerie Treyer^{1,3}, Junfeng Sun⁴, Chencheng Zhang⁵, Anton Gietl¹, Christoph Hock^{1,6}, Daniel Razansky², Roger M. Nitsch^{1,6}, Ruiqing Ni^{1,2,7},

for the Alzheimer's Disease Neuroimaging Initiative

¹Institute for Regenerative Medicine, University of Zurich, 8952 Zurich, Switzerland

²Institute for Biomedical Engineering, ETH Zurich & University of Zurich, 8093 Zurich, Switzerland

³Department of Nuclear Medicine, University Hospital of Zurich, University of Zurich, Zurich, Switzerland

⁴School of Biomedical Engineering, Shanghai Jiao Tong University, Shanghai, China

⁵Department of Neurosurgery, Center for Functional Neurosurgery, Ruijin Hospital, Shanghai JiaoTong University School of Medicine, Shanghai, China

⁶Neurimmune, Schlieren, Switzerland.

⁷Zentrum für Neurowissenschaften Zurich, Zurich, Switzerland

*A subset of the data used in preparation of this article were obtained from the Alzheimer's Disease Neuroimaging Initiative (ADNI) database (adni.loni.usc.edu). As such, the investigators within the ADNI contributed to the design and implementation of ADNI and/or provided data but did not participate in analysis or writing of this report.

Corresponding author: Dr. Ruiqing Ni, ruiqing.ni@uzh.ch

Address: Wagistrasse 12, 9th floor, 8952 Zurich, Switzerland

Text

Brain stimulation has been a potential nonpharmacological therapeutic intervention for a range of brain diseases. Different neuromodulation methods have been developed and applied to human brain imaging. The skull compartment exerts a strong influence on the imaging and stimulation results, suggesting the need to accurately examine its geometry and alterations in the population. Thinning and geometric changes in the skull may also occur due to aging and disease. Optimization of the probe location on the head for neuroimaging/brain simulation thus has added value in various neurostimulation and imaging studies, such as simulation ultrasonic wave propagation and acoustic transmission [1]. Computed tomography (CT) imaging has been used to investigate the changes in bone thickness. However, radiation exposure, particularly to the brain, is not ideal for volunteers or patients. Analysis using routine structural magnetic resonance imaging (MRI) data is a feasible alternative. Structural MRI-based automatic skull reconstruction from images was challenging, as compact bone has a very low signal in MRI. Recent efforts have enabled the development of accurate and automatic head segmentation/skull stripping pipelines from MRI for individualized head modelling [2, 3], which is not immediately applicable for skull analysis. Moreover, cortical thinning has been found to be associated with amyloid-beta and tau accumulation in Alzheimer's disease (AD) and prodromal AD, as well as in clinically normal older adults, and associated with increasing age. The changes in skull thickness and scalp-to-cortical distance (SCD) with age and sex have not been evaluated in a large cohort, which is relevant in brain stimulation applications.

Here, we developed an open-source fully automated pipeline BrainCalculator for the computation of the skull thickness map, and SCD, based on structural T₁-weighted (T₁w) MRI data from the Alzheimer's Disease Neuroimaging-Initiative (ADNI) [4] (available at <https://github.com/Junha0Zhang/BrainCalculator>). Next we assessed MRI-based skull

thickness in a group of 407 cognitively normal older adults (71.9 ± 8.0 years, 60.2% female) by using the developed pipeline (**STable.1**).

The original T_1w MRI file of the human head (.nii) from ADNI (**Fig.1a**) was processed by using BS Skullfinder to generate 3D meshes (.obj) for the cortical surface, scalp surface, and inner and outer skull surface (**Figs.1b-e**). All datasets were registered to the same coordinate. Brain volume was calculated based on the cortex surface of the brain (**Fig.1b**). Next, uniformly sampled points from the four surfaces for the cortex, scalp, inner and outer table (**Figs.1b-e**) were used to generate corresponding point clouds(.pcd) (**Figs.1f-i**). Earlier studies have used an exhaustive neighbor search of points [5]. To efficiently search for the nearest points, we used the K-dimensional tree algorithm to speed up the computation process[6]. For every point in the scalp and outer skull surface (**Figs.1g, i**), the closest point in its paired data (cortex/inner skull) was identified (**Fig.1k**). Next, we computed the skull thickness (**Fig.1j**) and SCD maps (**Fig.1l**) for all the selected points and regions. The skull thickness map is visualized, and the value is reported when the user selects the location on the skull by a cursor. The whole pipeline takes approximately 8 minutes for one dataset as tested on Dell-XPS15 (Intel i7-9750H CPU).

Next, we compared different open-source packages in the suitability and performance for automatic (without manual correction) skull segmentation and SCD computation. We demonstrated the utility of our BS-Skullfinder preprocessing based pipeline [7, 8] along with FSL-Brain Extraction Tool (FSL) 2 [9] and SPM12-based unified segmentation [10] for computing the skull meshes and thickness maps. SPM also provided probability maps for cerebral spinal fluid, white matter and gray matter, however did not provide scalp map. To evaluate the performance and compare the similarity of different analysis methods, we computed the Dice coefficients for each of the labels and the CT pair. CT data were used as ground truth. The Dice coefficient measures the similarity of two sets of data. Higher similarity

of the segmentation to the CT reference is indicated by the closeness to 1.0. We did not include the lower parts of the skull in the comparison, as they were either noisy or absent in the processing. We found that the three methods BS, FSL, and SPM generated globally similar segmentations for the skull and scalp mask using the T_{1w} MRI data (**STable.2, SFig.1**). However, mismatches in the temporal bone, sphenoid bone and occipital bone were observed in the automatically processed data based on FSL BET segmentation when overlaying the segmentation with CT (**SFigs.1c,g**). This mismatch could be observed in the skull thickness map generated based on FSL BET segmentation (**SFigs.1i,j**). Given the importance of the temporal bone, sphenoid bone and occipital bone regions in focused ultrasound stimulation and other neurostimulation approaches, BS-based segmentation was chosen in our automatic pipeline.

Next, we applied our analysis pipeline to compute the skull thickness map for the 407 T_{1w} MR datasets from ADNI (**STable.3, SFig.2**). There was a trend of higher skull thickness in male participants than in female participants, although the difference was not statistically significant. Significant skull thickening was found in the temporal bone of male participants in the 71-80-year-old group compared to the 60-70-year-old group. In the sphenoid bone of female participants, there was a slight increase associated with age ($r=0.1734, p=0.0066$). In other regions of skull bones, no correlation between age and skull thickness was detected in either sex. The magnitude of skull thickening was higher in the sphenoid bone and occipital bone of females than in those of males. We further computed SCD map for the same ADNI cohort (**STable.4, SFig.3**). We observed that in all the regions, there was an increased SCD associated with age in both the male and female groups. The slope of the increase in SCD was steeper in the female than in males in the temporal cortex and was comparable in other brain regions (**STable.4**).

In conclusion, we developed an open-source skull thickness and SCD analysis pipeline

for structural MR brain scans and demonstrated the association between skull thickness and SCD with age. The automatic efficient computation toolbox for skull thickness and SCD map analysis is potentially useful for personalized neurostimulation planning.

Conflict of Interest

The authors declare that the research was conducted in the absence of any commercial or financial relationships that could be construed as a potential conflict of interest.

Author Contributions

RN designed the study; JZ wrote the code; JZ and RN performed the analysis; VT, AG, JZ, and RN interpreted the data; and JZ and RN wrote the draft. All authors read and approved the final manuscript.

Funding

RN received funding from Helmut Horten Stiftung, Vontobel Stiftung, and Zentrum für Neurowissenschaften, University of Zurich.

Acknowledgements

Data collection and sharing for this project was funded by the ADNI (National Institutes of Health Grant U01 AG024904) and DOD ADNI (Department of Defense award number W81XWH-12-2-0012). ADNI is funded by the National Institute on Aging, the National Institute of Biomedical Imaging and Bioengineering, and through generous contributions from the following: AbbVie, Alzheimer's Association; Alzheimer's Drug Discovery Foundation; Araclon Biotech; BioClinica, Inc. ; Biogen; Bristol-Myers Squibb Company; CereSpir, Inc. ; Cogstate; Eisai Inc. ; Elan Pharmaceuticals, Inc. ; Eli Lilly and Company; EuroImmun; F.

Hoffmann-La Roche Ltd. and its affiliated company Genentech, Inc. ; Fujirebio; GE Healthcare; IXICO Ltd. ;Janssen Alzheimer Immunotherapy Research & Development, LLC. ; Johnson & Johnson Pharmaceutical Research & Development LLC. ; Lumosity; Lundbeck; Merck & Co., Inc. ; Meso Scale Diagnostics, LLC. ; NeuroRx Research; Neurotrack Technologies; Novartis Pharmaceuticals Corporation; Pfizer Inc. ; Piramal Imaging; Servier; Takeda Pharmaceutical Company; and Transition Therapeutics. The Canadian Institutes of Health Research is providing funds to support ADNI clinical sites in Canada. Private sector contributions are facilitated by the Foundation for the National Institutes of Health (www.fnih.org). The grantee organization is the Northern California Institute for Research and Education, and the study is coordinated by the Alzheimer's Therapeutic Research Institute at the University of Southern California. ADNI data are disseminated by the Laboratory for Neuro Imaging at the University of Southern California.

References

- [1] Attali D, Tiennot T, Schafer M, Fouragnan E, Sallet J, Caskey C, et al. Three-layer model with absorption for conservative estimation of the maximum acoustic transmission coefficient through the human skull for transcranial ultrasound stimulation. *Brain Stimul* 2022.
- [2] Puonti O, Van Leemput K, Saturnino GB, Siebner HR, Madsen KH, Thielscher A. Accurate and robust whole-head segmentation from magnetic resonance images for individualized head modeling. *Neuroimage* 2020;219:117044.
- [3] Nielsen JD, Madsen KH, Puonti O, Siebner HR, Bauer C, Madsen CG, et al. Automatic skull segmentation from MR images for realistic volume conductor models of the head: Assessment of the state-of-the-art. *Neuroimage* 2018;174:587-98.
- [4] Weber CJ, Carrillo MC, Jagust W, Jack CR, Jr., Shaw LM, Trojanowski JQ, et al. The Worldwide Alzheimer's Disease Neuroimaging Initiative: ADNI-3 updates and global perspectives. *Alzheimers Dement (N Y)* 2021;7(1):e12226.
- [5] Lillie EM, Urban JE, Lynch SK, Weaver AA, Stitzel JD. Evaluation of Skull Cortical Thickness Changes With Age and Sex From Computed Tomography Scans. *J Bone Miner Res* 2016;31(2):299-307.
- [6] Muja M, Lowe D. Flann-fast library for approximate nearest neighbors user manual. 2009.
- [7] Shattuck DW, Leahy RM. BrainSuite: an automated cortical surface identification tool. *Med Image Anal* 2002;6(2):129-42.
- [8] Dogdas B, Shattuck DW, Leahy RM. Segmentation of skull and scalp in 3-D human MRI using mathematical morphology. *Hum Brain Mapp* 2005;26(4):273-85.
- [9] Jenkinson M, Beckmann CF, Behrens TEJ, Woolrich MW, Smith SM. FSL. *NeuroImage* 2012;62(2):782-90.
- [10] Ashburner J, Friston KJ. Unified segmentation. *NeuroImage* 2005;26(3):839-51.

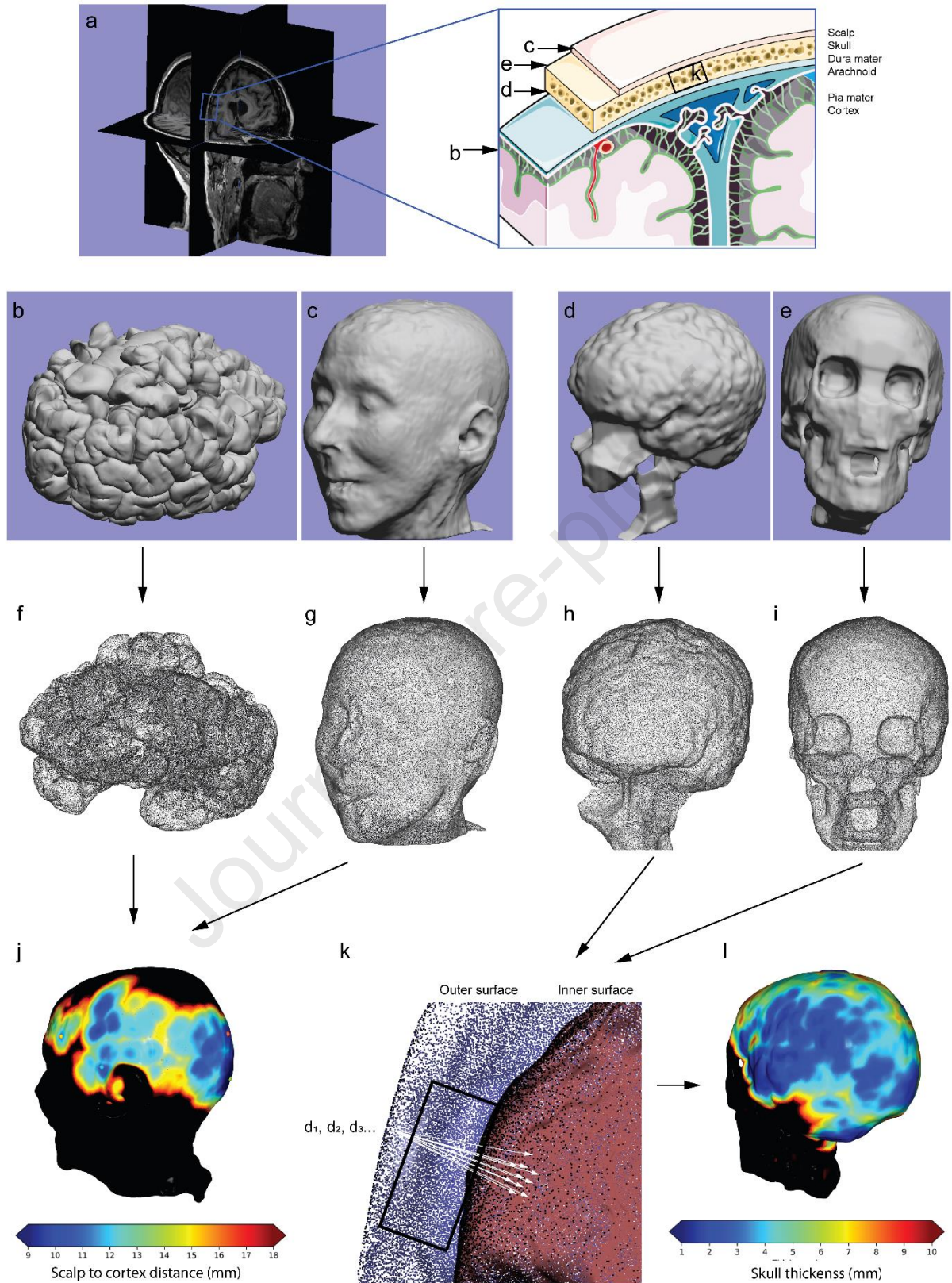
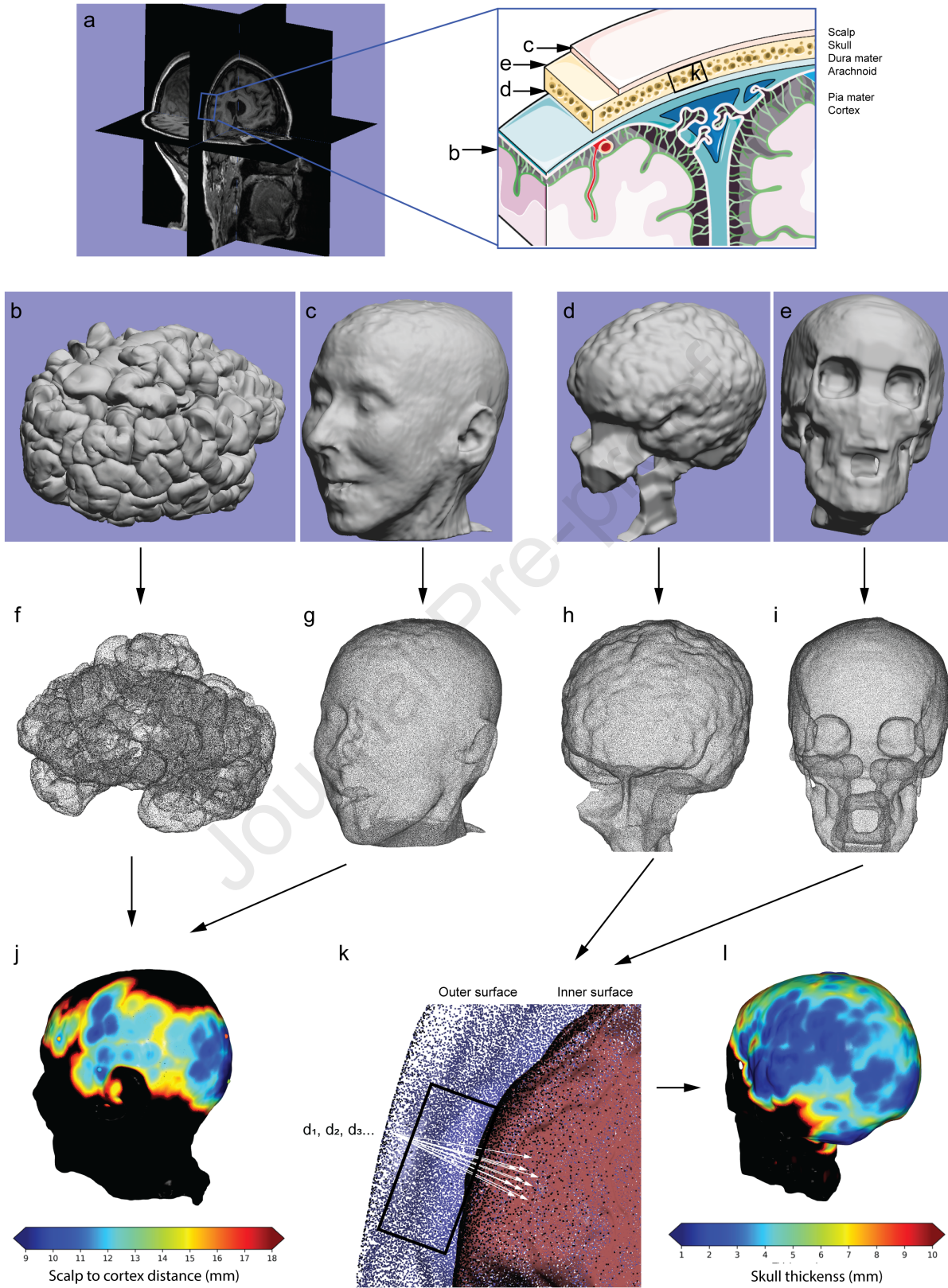


Fig. 1

Figure Legend

Fig. 1 Analysis pipeline for human skull thickness and scalp-to-cortex distance (SCD) using T₁w MRI data. (a) Original MRI file and zoom-in-view summarizing position of b-k; (b-i) Surfaces and corresponding point clouds for (b, f) cortex, (c, g) scalp, (d, h) inner skull and (e, i) outer skull; (j) SCD map. Scale bar = 9-18 mm (blue-red); (k) Zoomed-in view of the skull (in a) indicating the inner surface (red dots) and outer surface (blue dots). d_i is the i^{th} nearest point on the inner surface to each point on the outer surface (arrow line). (l) Skull thickness map. Scale bar = 1-10 mm (blue-red). Representative images based on T₁w MR from one 79-year-old male.



Declaration of interests

The authors declare that they have no known competing financial interests or personal relationships that could have appeared to influence the work reported in this paper.

The authors declare the following financial interests/personal relationships which may be considered as potential competing interests:

Journal Pre-proof